Hindawi
Advances in Civil Engineering
Volume 2022, Article ID 6951775, 12 pages
https://doi.org/10.1155/2022/6951775

Research Article

Insights into Optimal Schemes of Radial Network Arch Pedestrian Bridge

Rimantas Belevičius,[1] **Dainius Rusakevičius**,[2] **and Saulius Valentinavičius**[1]

[1]*Department of Information Technologies, Faculty of Fundamental Sciences, Vilnius Gediminas Technical University, Vilnius LT 10223, Lithuania*
[2]*Department of Applied Mechanics, Faculty of Civil Engineering, Vilnius Gediminas Technical University, Vilnius LT 10223, Lithuania*

Correspondence should be addressed to Rimantas Belevičius; rimantas.belevicius@vgtu.lt

Received 29 March 2022; Revised 14 June 2022; Accepted 31 October 2022; Published 17 November 2022

Academic Editor: Vagelis Plevris

The main objective of the article is to find the optimal ranges of the cardinal topological, shape, and dimensional parameters that fully describe the constructional scheme of pedestrian radial network arch bridges of moderate spans. This task is solved by formulating the global optimization problem and seeking the minimum mass of the whole bridge structure. An optimal bridge scheme was obtained by tuning a large set of interdependent design parameters of diverse character: the topological parameters–the type of hanger arrangement, and the number of hangers; the shape parameters–hanger spread and central section angles, the alteration of these angles, and the arch rise; and the sizing parameters–all cross-sectional dimensions of structural members. Mathematically, this is a constrained mixed-integer global optimization problem solved by a stochastic evolutionary algorithm. Plane light-deck bridges of typical moderate 30, 45, 60, 75, and 90 m spans were optimized. Decisive design parameters and their rational ranges for all spans were revealed. In addition, the effects of some simplifications of the general bridge scheme were shown: using the constant spread and central section angles; imposing certain values on the ratio arch rise/bridge span; bounding the hanger diameters to a given value; and so on. Obtained results clearly indicate that the design recommendations for the lightweight network arch bridges should differ from the recommendations for similar automotive and railway bridges. Our findings are: the optimal ratio of arch rise to the bridge span is 0.20–0.30, the number of hangers is >40 even for the shortest spans, the spread angle between hangers is 30°–40°, and the girder mass amounts to ~30% of the total bridge mass, while the mass of hangers amounts up to 20% and increases when imposing constraints on the minimal radius at the expense of diminishing arch mass.

1. Introduction

The original ideas of the radial network arch scheme for bridges are found in the pioneering works of engineer Octavius F. Nielsen, published in the early 20th century [1, 2]. The bridges of O. F. Nielsen's scheme had inclined but not crossing hangers. Later, in the 6th decade, Per Tveit and his co-workers [3, 4] showed that a scheme with hangers with multiple crossings lets avoid compression of hangers and therefore is more efficient. Many railways and automotive bridges based on this scheme were built in Norway, Germany, the United States, and other countries.

The behaviour of such bridges was analysed in several scientific papers [2, 5–9] where some optimal ranges of the parameters on the constructional elements of the bridges were suggested. Thus, Schanack [9–11] studied a bridge scheme with a circular arch and obtained the rational range of spread angles between neighbouring hangers. Next, Teich [2, 7, 8] searched for the optimal shape of the arch and gave recommendations for the optimal spread angle values for four different hanger arrangement schemes and for the optimal number of hangers. One of the most important constructional parameters is the ratio between the rise of the arch and the span of the bridge; some considerations on this

are given in [4]. Several papers analysed the behaviour of already built bridges [1, 2, 4, 9].

Generally, it is shown that the radial network arch bridges with multiple crossing hangers are the most effective among different network schemes of bridges if the bending moments in the arch and the axial forces in the hangers are considered [12] and also are less vulnerable to the accidental cable loss events [13].

Usually, the cited works concentrate on finding optimal values for some constructional parameters of the bridge scheme, taking as the objective function the minimum bending moments or the minimum stresses in the elements of the bridge. Thus, Ostrycharczyk and Malo [6, 14] performed 19,200 variant calculations of a 2D network arch scheme with different radial hanger arrangements, changing the arch rise and the hanger spread angles α [Figure 1] in the diapason from 0 to 70°. They obtained minimal bending moments at the angle values $\alpha = 42–55°$. Similar problems were investigated by Islam Ahsan and Ahsan [15, 16], and Pipinato [17, 18]. Islam Ahsan showed that circular arch network bridges compared to parabolic arch bridges have a lower arch rise and a lesser number of hangers. Also, they obtained slightly different optimal spread angles: $\alpha = 32–40°$.

Nowadays, several works investigate different behavioural aspects of network arch bridges based on detailed nonlinear analyses. Bruno et al. [13] identified the main factors reducing the risk of accidental cable loss for 2D bridge frames. Ammendolea et al. [19] expanded the investigations to the 3D bridge scheme. Tetougueni et al. [20, 21] explored the lateral response of the 3D bridge against traffic loads, while the works of Greco et al. [22–24] are dedicated to the investigation of out-of-plane instability effects due to vertical loads and to the influence of different bracing systems between bridge arches on the instability strength.

All this research concerns the network arch bridges for railway and automotive transport. Today, network arch bridges are often used also for pedestrian traffic. Since these bridges usually have smaller spans and lesser loadings, the design recommendations for railway and automotive bridges are not fully applicable to them. Some considerations for the analysis of pedestrian network arch bridges can be found in [25–28]. In Belevičius et al. [29, 30] the scheme of the pedestrian network arch bridge was optimized changing all main constructional parameters simultaneously: the arch rise, the number of hangers, their inclination and spread angles, and all cross-sectional dimensions of bridge elements under different loading conditions. The number of design parameters is large; and therefore, the mathematical optimization problem was formulated and solved using stochastic global optimization algorithms. In [31] the pedestrian bridge scheme of a 60 m span was investigated in detail, while [32] provides the optimal structural parameters of this bridge at different optimization conditions and some fixed values of structural parameters.

This paper attempts to generalize the findings on optimal diapasons of constructional parameters of pedestrian radial network arch bridges for different spans of 30, 45, 60, 75, and 90 m, which are typical for moderate pedestrian bridges. The arch in all cases is circular. The bridge is investigated in two dimensions, i.e., only one of the two parallel bridge frames is optimized assuming that bracing between frames assures the out-of-plane stability of the bridge. We try to find the optimal parameters of the bridge scheme by pursuing the minimal bridge mass. Besides, the paper shows how the additional constraints on the bridge parameters, such as the fixed ratio of bridge rise to the span, fixed hangers' spread angles, fixed hanger diameters influence the bridge mass. This paper is organized as follows: Section 2 provides the formulation of the optimization problem, Section 3 shortly describes the optimization technique using stochastic evolutionary algorithms, and the 4th Section discusses the results of optimization. Some recommendations on the design of pedestrian bridges of the studied type are given in the conclusions.

2. Methodology

2.1. Optimization Problem. Figure 1 shows the general scheme of the bridge frame under consideration along with the main design parameters: the arch rise f, the number of sections, the spread and central section angles α and β, and the cross-section characteristics of the arch, girder, and hangers. The radius of an arch is determined by the arch rise and span: $R = L^2 + 4^* f^2/8^* f$. All design parameters along with their bounds and characteristics are listed in Table 1. Figure2 explains the algorithm of scheme generation.

The optimization problem is formulated in the following equation:

$$F^* = f(\mathbf{x}^*) = \min_{x \in D} f(\mathbf{x}), \tag{1}$$

for all load cases subject to the following points:

(i) Structural equilibrium constraints.

(ii) Strength constraints on all structural elements.

(iii) In-plane stability constraints on the arch elements.

(iv) "Deadly penalty" for the occasion of compression in any hanger.

(v) Vertical deck displacements' constraints.

$f(\mathbf{x})$ in equation (1) is a nonlinear objective function of continuous and integer variables $f: \mathfrak{R}^n \longrightarrow \mathfrak{R}$, where n is the number of design parameters $\boldsymbol{x}$, and $D \subset \mathfrak{R}^n$ defines the feasible space of design parameters. The global minimum F^* and minimizer $\mathbf{x}^*$: $f(\mathbf{x}^*) = F^*$ should be found. It is assumed that the problem may have several local minima; the optimization results obtained clearly show the multiextrema character of the problem.

The total mass of the bridge is the objective function. The constrained optimization problem is transformed into an unconstrained problem using static penalties proportional to the extent of constraint violation.

The structural equilibrium constraints are assured by solving the static problem via the original finite element method (FEM) program written by the authors. All strength, stability, and displacement constraints are formulated according to Eurocodes.

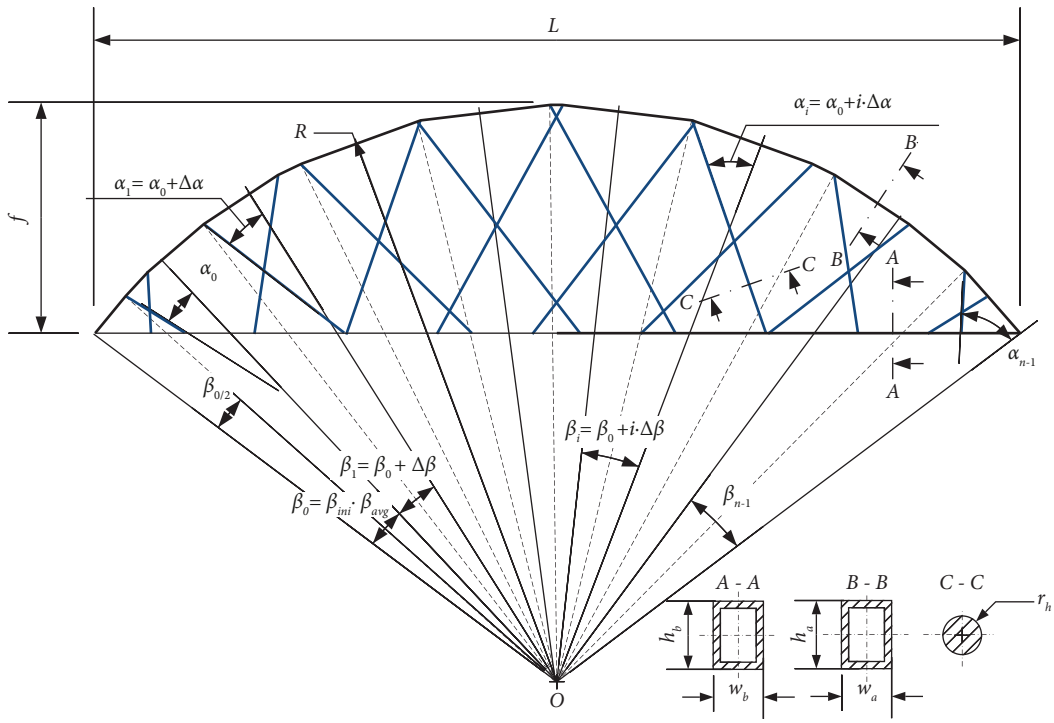

Figure 1: Bridge scheme with the main design parameters.

Table 1: Set of design parameters.

No. of a parameter	Parameters	Types	Lower bounds		Upper bounds	
			For varying angles	For constant angles	For varying angles	For constant angles
1	Arch rise f (m)	Continuous	$L/10$		$L/2$	
2	Number of sections (n)	Integer	5		40	
3	Spread angle α (°)	Continuous	5	5	35	45
4	Central section angle β (°)	Continuous	1.1		54	
5	Augment $\Delta\alpha$ (°)	Continuous	0.	0.	2.5	0.
6	β_{ini}	Continuous	0.5	1.0	1.5	1.0
7	Height of girder cross-section, h_b (m)	Continuous	0.1		1.0	
8	Width of girder cross-section, w_b, (m)	Continuous	0.08		0.4	
9	Height of arch cross-section, h_a (m)	Continuous	0.1		1.0	
10	Width of arch cross-section, w_a, (m)	Continuous	0.08		0.4	
11	Radius of hanger, R, (m)	Continuous	0.005		0.05	

The following problem idealizations are taken as follows:

(i) Linear finite element static analysis of the bridge scheme is performed. The linear solution is sufficient since the vertical displacements of the bridge girder are limited via optimization constraints.

(ii) The load-bearing structure of the bridge is composed of two parallel plane frame systems. Only one plane frame is analysed.

(iii) The dimensions of cross-sections of the arch and girder are constant along the whole length since the bridges under consideration are of moderate spans.

(iv) The arch and the girder are made of rectangular hollow tubes. The thickness of the tube wall depends on the height and width of the profile and is chosen to ensure the local stability of the cross-section.

(v) All hangers are made of round solid profile. The diameter of all hangers in the scheme is the same.

(vi) The dimensions of cross-sections of the arch, girder, and hangers are taken as continuous

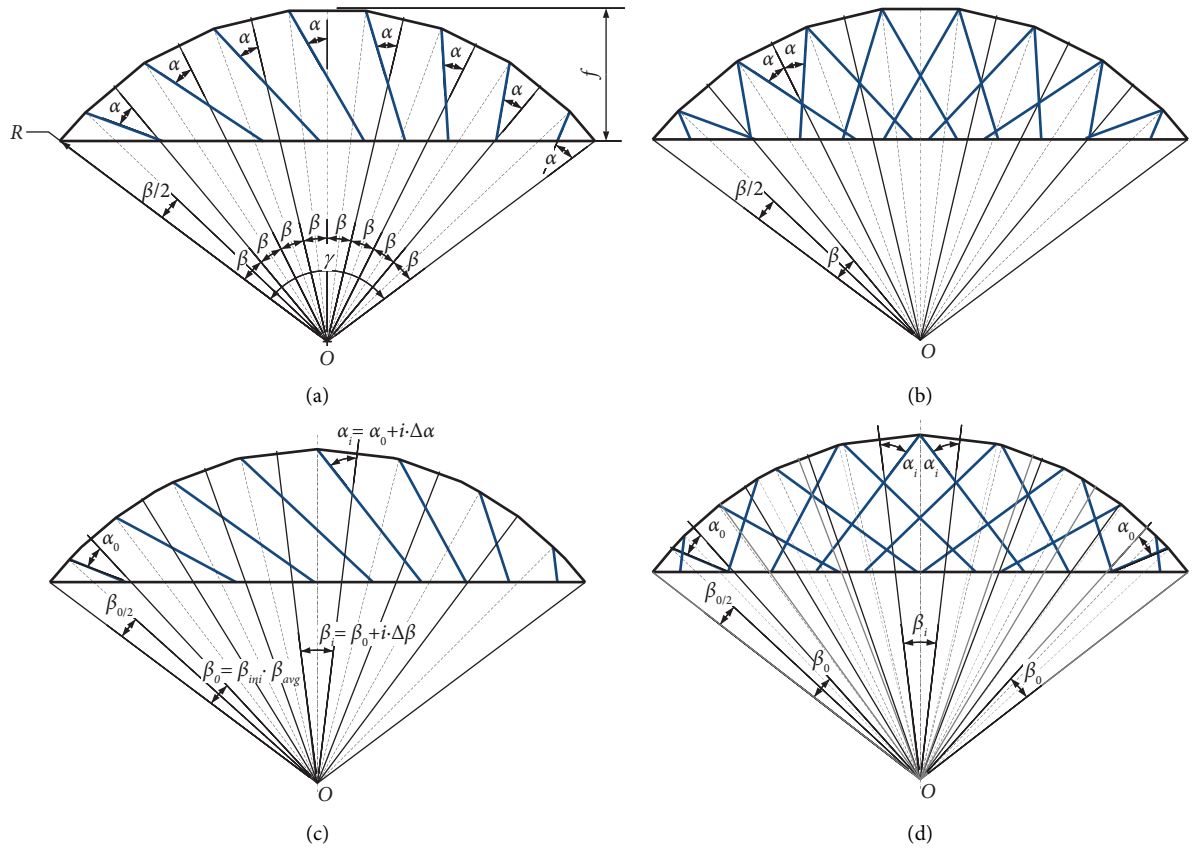

Figure 2: Algorithm of the bridge scheme generation: (a) Initial scheme of hangers at constant angles α and β, (b) Final scheme–obtained by the mirror image; (c) and (d) the same schemes at varying angles.

variables since the use of assortment table profiles considerably constricts optimization [28].

(vii) The material of all structural elements is steel S355.

(viii) All structural elements including hangers and slightly distorted arch elements are idealized as 2-node beam finite elements with 12 degrees of freedom.

(ix) The connections between structural elements are perfectly rigid.

The optimization problem was solved for four load cases. Each load case includes the self-weight of the bridge structure itself, permanent (dead) loading evenly distributed along the span on the girder of the bridge, and variable (traffic) loading. The permanent loading depends on the type of bridge deck and is taken from 7.5 to 10 kN/m. The intensity of variable loading is from 2.5 to 5 kN/m^2 according to Eurocodes EN 1991-2 which is equivalent under consideration from 7.5 to 15 kN/m for the bridge scheme. The first loading case consists of the permanent loading plus traffic loading applied on the whole span [Figure 3(a)]. The next three load cases (Figure 3(b)) include permanent loading plus variable loading on half of the span since this is usually the critical case for buckling [33]. To keep the thrust force in the arch more or less constant thus assuring the correct analysis results [31], the following relation is employed:

$H = g \bullet (1 + 0.5 \bullet \gamma) \bullet L^2/8 \bullet f$, where H is the thrust force in the arch, g is the permanent load, γ is the ratio between variable load v and permanent load g. Thus, for all asymmetric loading cases and taking the ratio $\gamma = 1.0$, 1.50, and 2.0, the loads' intensities as shown in Figure 3 were obtained.

2.2. Optimization Technique. After the global optimization stochastic evolutionary algorithm (EA) from MathWorks [34] randomly creates the initial population of design parameters sets, the optimization problem is solved in four steps:

(i) Original meshing program written by authors based on the values of design parameters prepares the whole finite element mesh of the bridge frame herewith calculating the loadings on the mesh nodes and imposing the boundary conditions.

(ii) Original finite element program solves the linear static problem. The computation time is a bottleneck in global optimization problems; therefore, we cannot rely on the more detailed nonlinear analysis or use the commercially available finite element packages; instead the fast problem-oriented Fortran program written by the authors is employed.

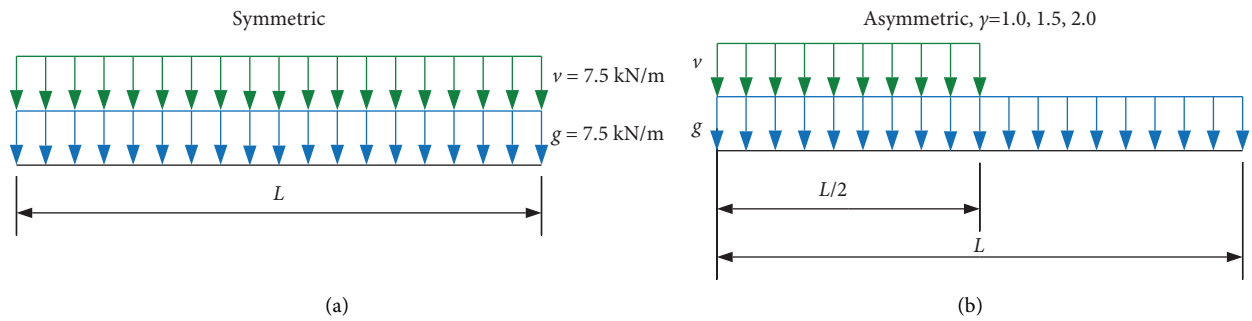

Figure 3: Loading cases and intensities of variable and permanent loadings. (a) Symmetric loadings, (b) Asymmetric loadings: at $\gamma = 1.0$ $v = g = 10.0$ kN/m; at $\gamma = 1.50$ $v = 12.86$ kN/m, $g = 8.57$ kN/m; at $\gamma = 2.0$ $v = 15$ kN/m, $g = 7.5$ kN/m.

(iii) Original program obtains the objective function value, verifies the constraints, and penalizes the objective function in case of a constraint violation.

(iv) Based on the results obtained, EA generates the new improved population of design parameter sets.

Exhaustive details on the optimization technique can be found in [31].

The design parameters set is chosen so that it could determine the complete finite element mesh of the bridge frame together with all physical properties of structural elements of the frame. The most discussed topic in the radial network arch bridge geometry is the hanger arrangement scheme. We suggest the following algorithm, which allows obtaining the arbitrary radial hanger arrangement scheme. Two symmetrical sets of hangers are combined where two independent angles–the hanger spread angle α and the central section angle β determine the positions of the hangers. Figures 2(a) and 2(b) show the initial set of hangers and the final obtained scheme when the angles α and β are constant. Figures 2(c) and 2(d) show the general scheme when both angles change constantly. For the alternating central section angle instead of the angle augment, it is handier to formulate the ratio of the initial central section angle β_{ini} to the average angle β_{avg}. Denoting the total section angle by γ and the number of sections by n (the total number of hangers then is $2n$), the central section angle augment is obtained via the following equation:

$$\beta = 2\frac{\gamma - n \cdot \beta\text{avg} \cdot \beta\text{ini}}{n \cdot (n-1)}. \quad (2)$$

Table 1 provides a complete list of design parameters along with their bounds for all bridge spans L.

3. Results and Discussion

Bridges of five different spans were optimized: 30, 45, 60, 75, and 90 m. The loading on each bridge consists of the same four loading cases, and the loading intensities are also the same.

The results in Figures 4–6 show, first of all, the quality of the optimization procedure. Here, the best five optimized values of the main parameter of the bridge scheme–the ratio of arch rise to the span are shown for all five optimized bridge schemes. Figure 4 compares the obtained ratio values at the full set of optimization parameters vs. at the reduced set of parameters excluding variation of spread and central section angles. As expected, a wider set of optimization parameters conditions a bigger scattering of results (denoted in the legend as α, β var), however, at close values of the total bridge mass. Figures 5 and 6 show the same dependencies at fixed values of hanger radii: $R \geq 10$ mm and $R \geq 20$ mm, correspondingly. These inequality constraints turn during the optimization procedure indeed into equality constraints: the optimization procedure always ends up with the lower values of radii, i.e., 10 and 20 mm.

When the variation of both angles is allowed, the optimal values of the ratio f/L are always higher than at the constant angles. This is seen from Figures 7(a) and 7(b): the first figure shows the average optimized values at variable angles, while the second–at constant angles. It is interesting that the optimal ratio value at the full set of optimization parameters is about 0.29 and slightly increases with the span. Imposing additional constraints on the bridge scheme–limiting the hanger radii to 10 and 20 mm determines lower ratio values: about 0.23 and 0.21, respectively (Figure 7(a)). The dependencies retain the same character at both constant spread and central section angles, but at even lower values (Figure 7(b)).

Figures 8(a)–8(c) show how the fixed values of ratio f/L affect the total mass of the bridge scheme. We show only the marginal cases of dependencies for the spans of 30, 60, 75, and 90 m at the full set of optimization parameters, and at the constant angles α and β. All other remaining cases of optimization parameters' sets demonstrate the same character of dependencies. The range of ratio values from 0.16 to 0.40 with an augment of 0.04 is explored (but in the case when the total mass increase is evident, the optimization is stopped at the margin of 0.32). The dot with a black rim shows the absolute minimum in the curve. Thus, at the full set of optimization parameters (of course, excluding the arch rise f) the curve is always flatter-adaptability of remaining optimization parameters assures low losses in the objective function. By reducing the set of optimization parameters, the curves obtain a steeper profile. Longer and thicker hangers obtained along with increasing ratio f/L and the constraint on the radii of hanger results evidently in the increased total mass of bridge (Figures 8(a)–8(d)).

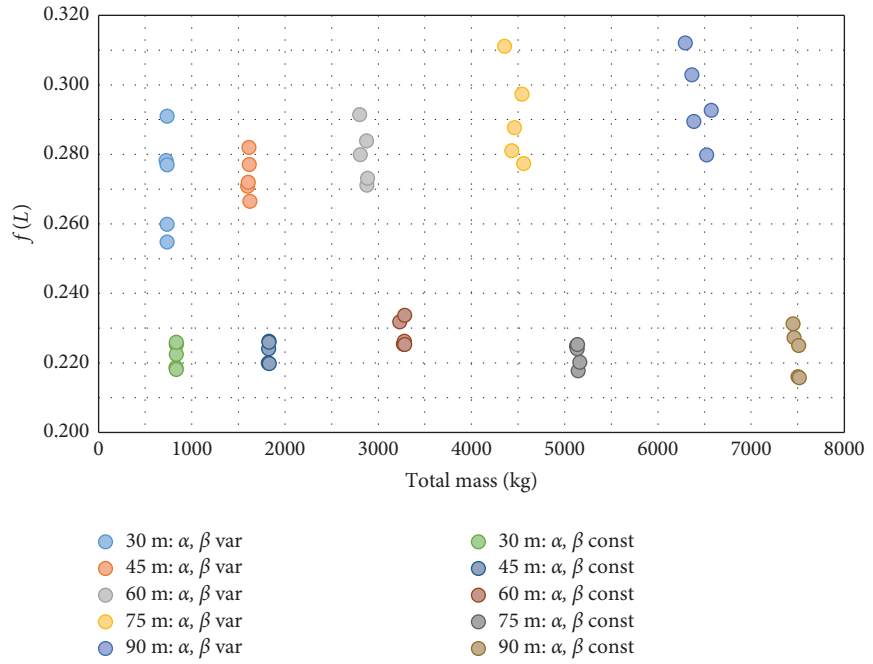

Figure 4: Five best values of ratio f/L at variable and constant angles α and β for all spans.

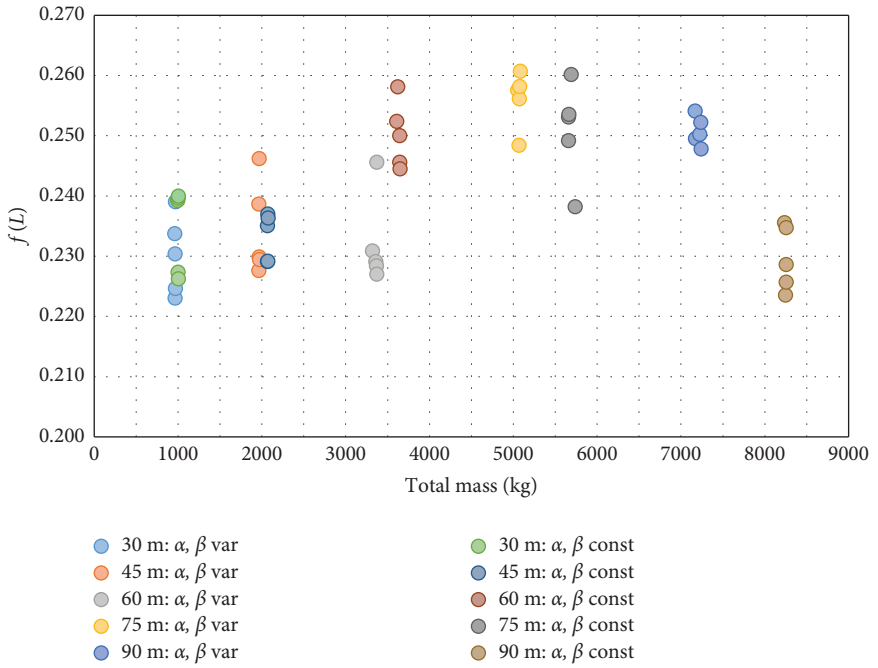

Figure 5: Five best values of ratio f/L at variable and constant angles α and β for all spans, and $R \geq 10$ mm.

Now, let us explore the parameter, recommendations on which in the literature are contradictory: the optimal number of the hangers. Due to the logic of bridge scheme generation, instead of hangers' number, the number of sections in the span will be shown; the number of hangers is twice as much. Figure 9 illustrates that the optimization algorithm ends up with rather scattered optimal values of this parameter at close values of the objective function.

Figures 10(a) and 10(b) show the average values of the number of sections n in the five best solutions at different sets of optimization parameters. Naturally, n increases with the bridge span and diminishes with increasing hanger radius. What is interesting, the n at constant angles α and β is always higher in all optimization cases.

Our bridge scheme generation algorithm allows obtaining schemes with constantly changing spread and

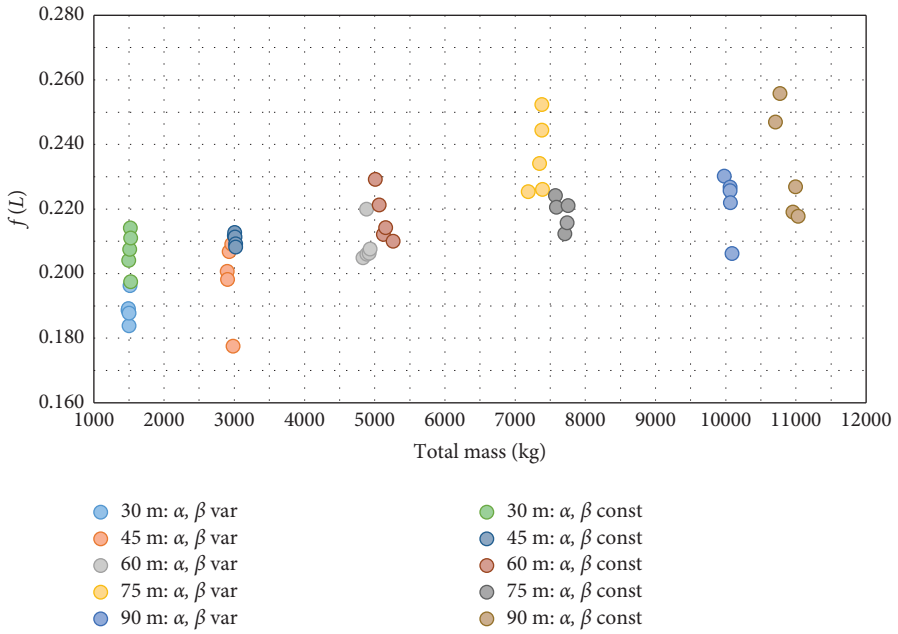

Figure 6: Five best values of ratio f/L at variable and constant angles α and β for all spans, and $R \geq 20$ mm.

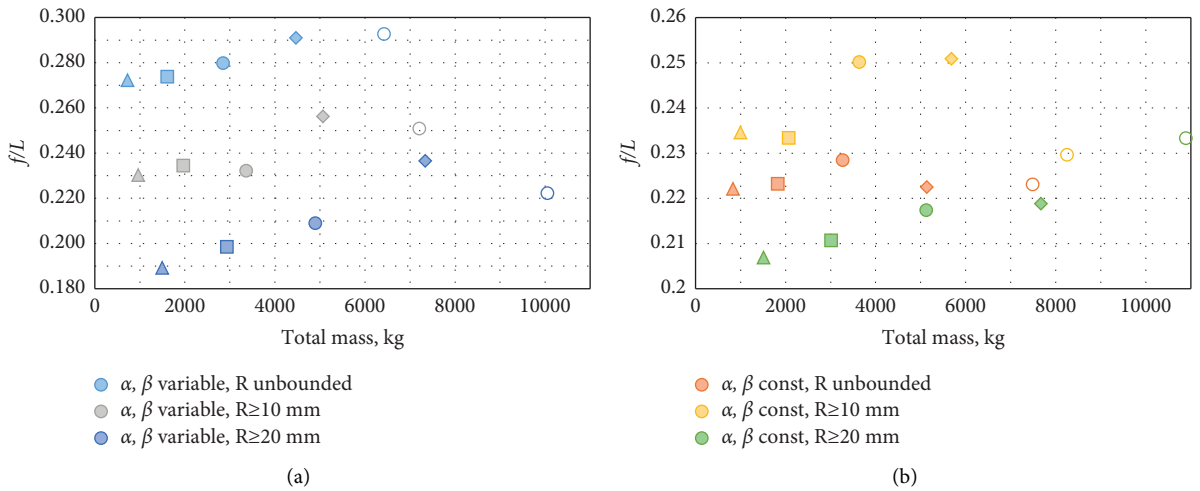

Figure 7: Average optimal values of f/L for all spans. (a) α, β variable. (b) α, β constant.

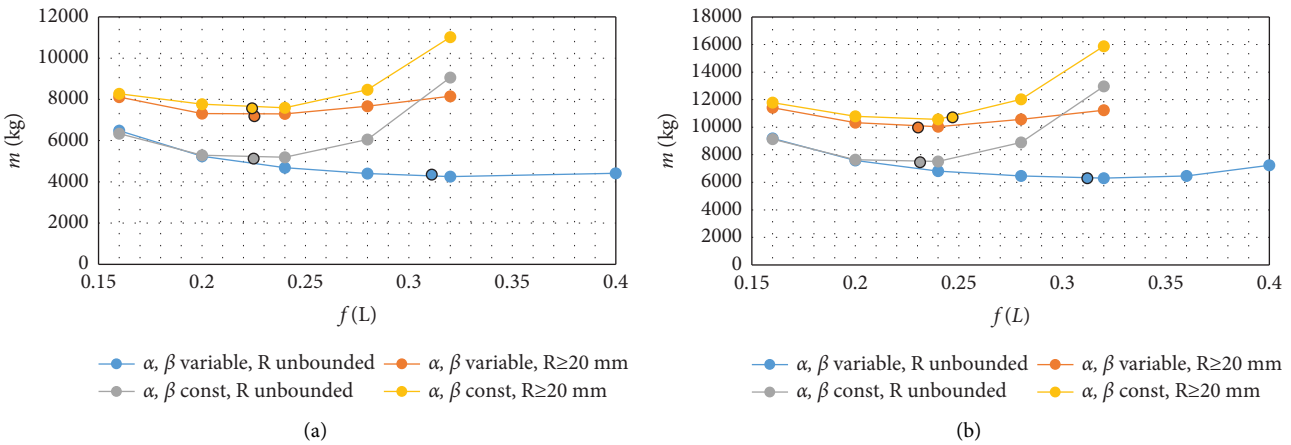

Figure 8: Continued.

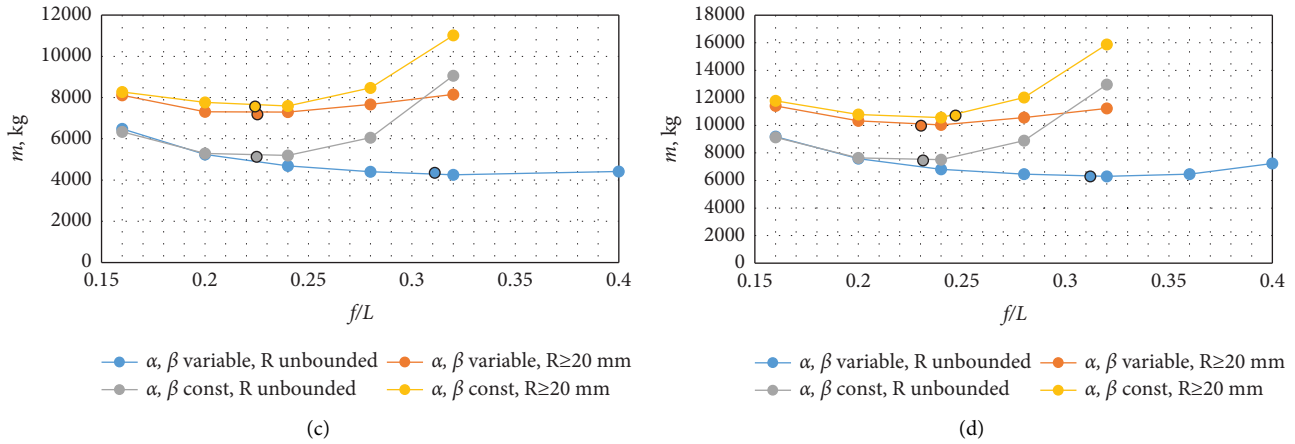

Figure 8: Dependency of total bridge mass to fixed ratio f/L: (a) 30 m span, (b) 60 m span, (c) 75 m span, and (d) 90 m span.

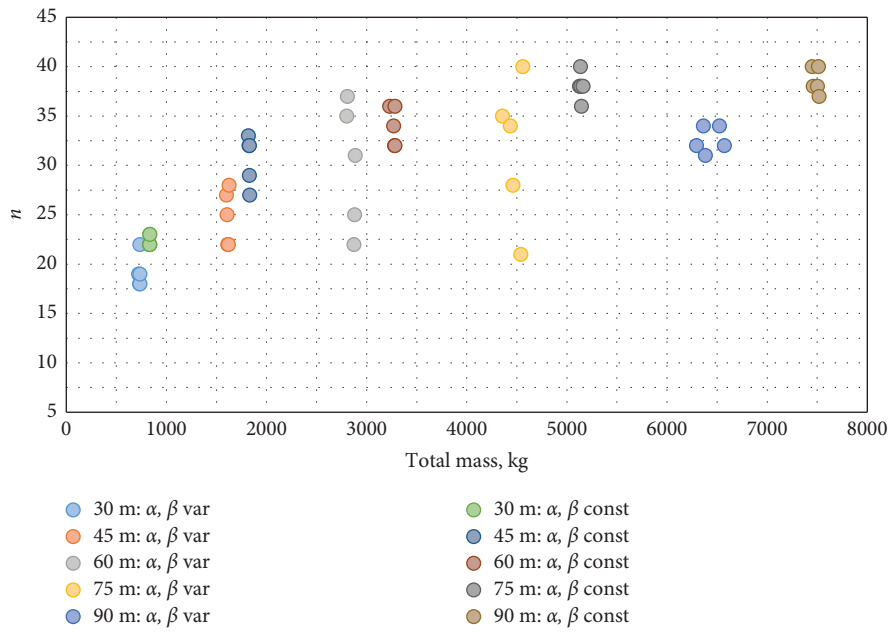

Figure 9: Five best values of section number n at variable and constant angles α and β for all spans.

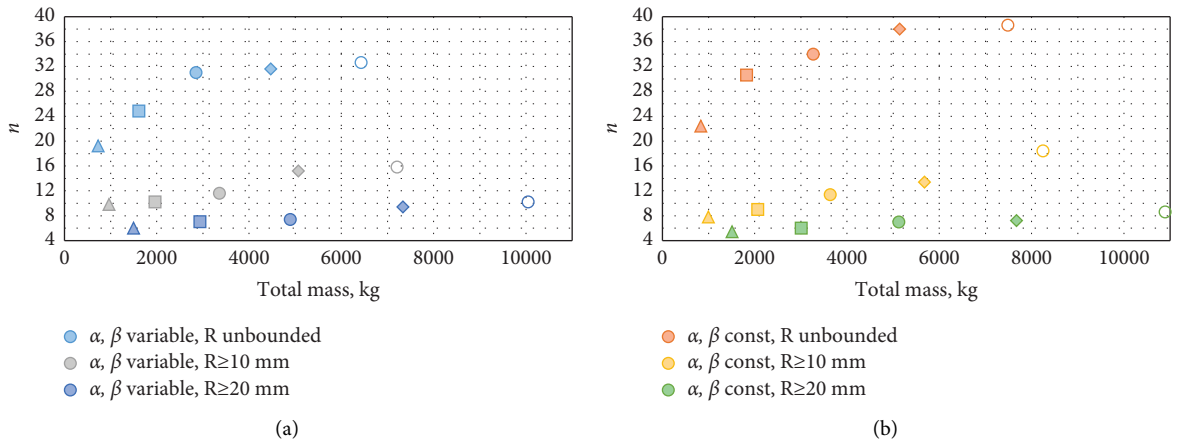

Figure 10: Average values of section number n: (a) α, β variable and (b) α, β constant.

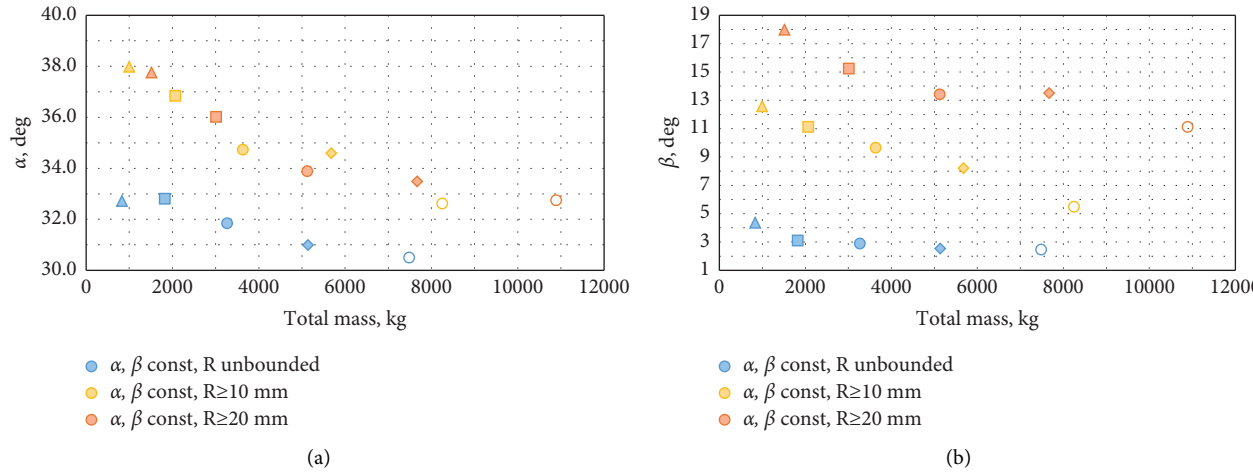

Figure 11: Average values of spread and central section angles for all spans: (a) α and (b) β.

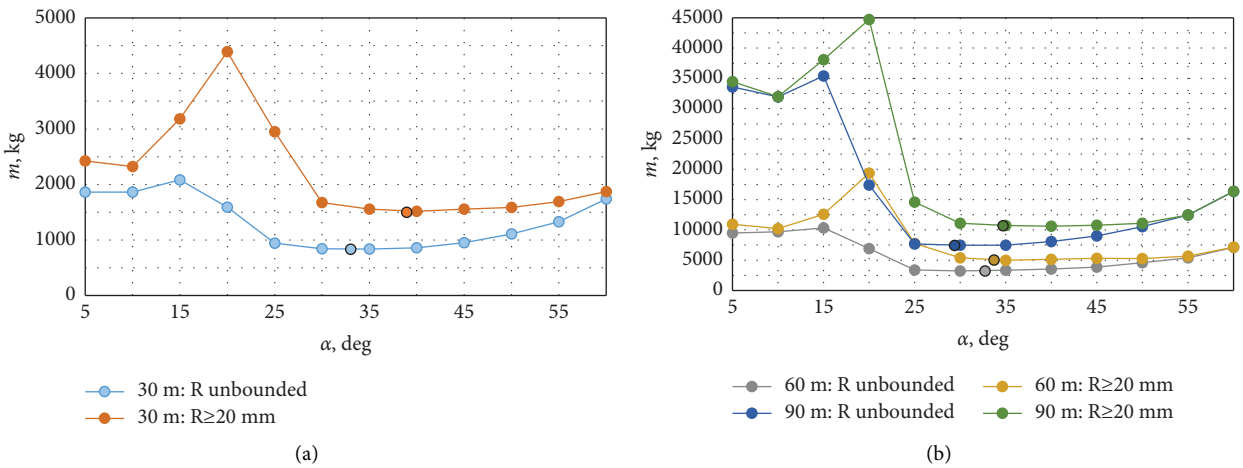

Figure 12: Dependencies of the total bridge mass on the fixed spread angle values for three spans of the bridge.

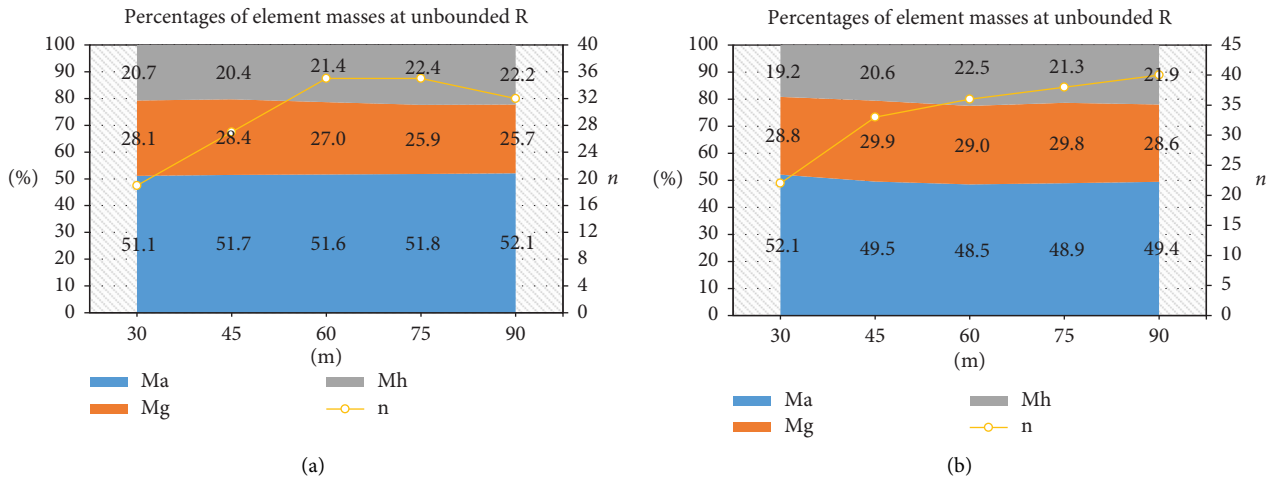

Figure 13: Continued.

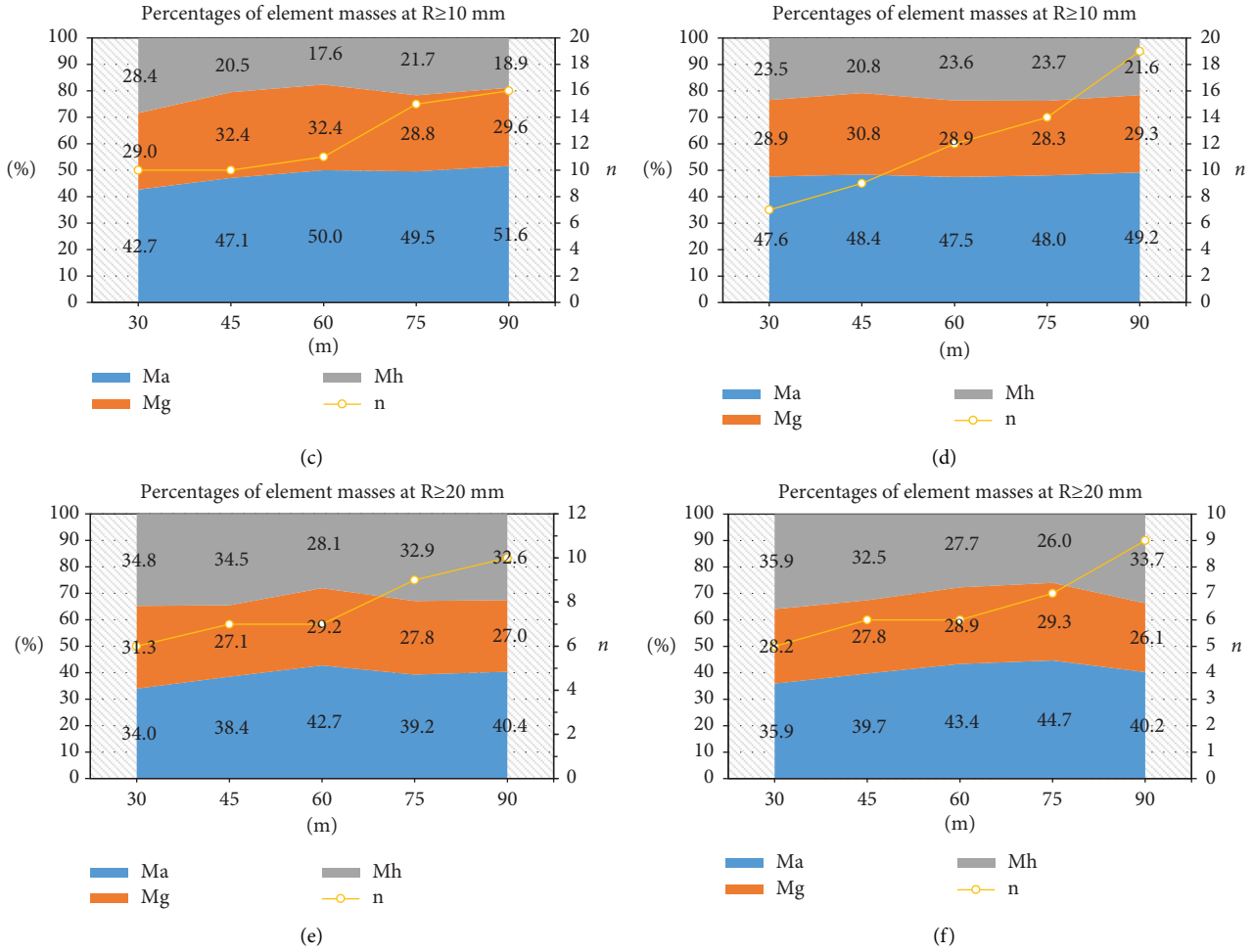

FIGURE 13: Distribution of mass between arch, girder, and hangers M_a, M_g, M_h and the number of sections n: (a), (c), (e)—at variable angles α and β; (b), (d), (f)—at constant angles α and β.

central section angles α and β. It was shown in [29] that a variable angle β has a slight impact on the mass of the bridge: excluding variation of the angle for a 60 m bridge, the mass increases up to 4%. Therefore, the main attention is given to the dependencies relative to the spread angle. Figure 11 provides the average optimal values of α and β in the five best solutions for all spans when both α and β are constant.

Figure 12 illustrates the influence of the spread angle on the total mass of the bridge scheme for two marginal cases of hanger radii: unbounded radius, and $R \geq 20$ mm, and three spans. If the angle has a low impact on the mass for a short span, with increasing span the influence becomes substantial. For comparison, the dots with black rims denote optimal values of the angle obtained optimizing the scheme with variable α.

As to the distribution of mass between structural elements in the optimal bridge schemes, despite the different hanger numbers, the total hanger mass is surprisingly stable for all spans [Figure 13]. However, taking thicker than needed hangers, i.e., $R \geq 10$ or 20 mm, the hanger mass' part increases–simultaneously with increasing total mass of the whole bridge. This clearly indicates that an optimal bridge scheme should have a larger number of thinner hangers. It is also evident, the largest part of the material should be amassed in the arch of the bridge.

The results and discussion may be presented separately or in one combined section, and they may optionally be divided into headed subsections.

4. Conclusions

Based on the results of mass optimization of pedestrian steel network arch bridges with radial hanger arrangements of moderate spans of 30, 45, 60, 75, and 90 m, we can conclude that the published design recommendations for corresponding automotive and railway bridges are not fully suitable for pedestrian bridges with lower loadings. Our findings are as follows:

(i) The optimal ratio of arch rise to bridge span for pedestrian bridges is approximately 0.20–0.30. In this range the sensitivity of the total bridge mass to the ratio is low.

(ii) The optimization always ends up with a large number of slender hangers (>40) even for the shortest spans.

(iii) The optimal range of spread angle between hangers is 30°–40°. Smaller spread angles, especially for the wider bridge spans, determine a substantial increase in bridge mass.

(iv) ~30% of the bridge mass should be amassed in the girder.

(v) ~20% of the bridge mass should be amassed in the hangers; imposing a constraint on the minimal hangers' radius increases the hangers' mass at the expense of diminishing arch mass.

Data Availability

All data on optimized parameters' values of all analysed bridge schemes as well as finite element solution results in a format similar to [32] can be obtained by request from the corresponding author.

Disclosure

This research was performed as part of the employment of the authors in Vilnius Gediminas Technical University.

Conflicts of Interest

The authors declare that there are no conflicts of interest regarding the publication of this paper.

References

[1] K. Geißler, U. Steimann, and W. Graße, "Netzwerkbogenbrücken – Entwurf, Bemessung, Ausführung," *Stahlbau*, vol. 77, no. 3, pp. 158–171, 2008.

[2] S. Teich, "Die Netzwerkbogenbrücke, ein überaus effizientes Brückentragwerk – tragwirkung und Konstruktion," *Stahlbau*, vol. 74, no. 8, pp. 596–605, 2005.

[3] W. Graβe, S. Teich, P. Tveit, and S. Wendelin, "Network Arches for Road Bridges," *Arch Bridges Arch'04*, pp. 1–10, CIMNE, Barcelona, Spain, 2004.

[4] P. Tveit, "Comparison of Steel Weights in Narrow Arch Bridges with Medium Spans (Vergleich der Stahlgewichte von schmalen Bogenbrücken mit mittleren Spannweiten)," *Stahlbau*, vol. 68, no. 9, pp. 753–757, 1999.

[5] R. M. Larssen, "The network arch – a slender and transparent bridge structure," in *Proceedings of the Nordic Steel 2012 Construction Conference*, pp. 249–259, Oslo, Norway, Europe, September 2012.

[6] A. W. Ostrycharczyk and K. A. Malo, "Parametric study of radial hanger patterns for network arch timber bridges with a light deck on transverse crossbeams," *Engineering Structures*, vol. 153, pp. 491–502, 2017.

[7] S. Teich and S. Wendelin, "Vergleichsrechnung einer Netzwerkbogenbrücke unter Einsatz des Europäischen Normenkonzeptes," *Diplomarbeit*, Technische Universität Dresden, vol. 38, 2001.

[8] S. Teich, "Entwicklung allgemeiner Entwurfsgrundsätze für Hängernetze von Netzwerkbogenbrücken," *Stahlbau*, vol. 80, no. 2, pp. 100–111, 2011.

[9] F. Schanack, "Berechnung der Knicklast in bogenebene von Netzwerkbögen," *Bautechnik*, vol. 86, no. 5, pp. 249–255, 2009.

[10] B. Brunn and F. Schanack, "Calculation of a double track railway network arch bridge applying the European standards," *Technische Universität Dresden*, vol. 20, pp. 68–72, 2003.

[11] B. Brunn, F. Schanack, and U. Steimann, "Network arches for railway bridges," in *Arch Bridges IV Advances in Assessment, Structural Design and Construction*, P. Roca and C. Molins, Eds., pp. 671–681, CIMNE, Barcelona, Spain, 2004.

[12] C. Pellegrino, G. Cupani, and C. Modena, "The effect of fatigue on the arrangement of hangers in tied arch bridges," *Engineering Structures*, vol. 32, no. 4, pp. 1140–1147, 2010.

[13] D. Bruno, P. Lonetti, and A. Pascuzzo, "A numerical study on network arch bridges subjected to cable loss," *International Journal of Bridge Engineering (IJBE)*, vol. 6, no. 2, pp. 41–59, 2018.

[14] A. W. Ostrycharczyk and K. A. Malo, "Parametric study on effects of load position on the stress distribution in network arch timber bridges with light timber decks on transverse crossbeams," *Engineering Structures*, vol. 163, pp. 112–121, 2018.

[15] N. Islam and R. Ahsan, "Optimization of hanger arrangement of network arch bridges," in *IABSE-JSCE Joint Conference on Advances in Bridge Engineering-II*, O. Amin and Bhuiyan, Eds., pp. 1–10, IOP Publishing, Dhaka, Bangladesh, 2010.

[16] N. Islam, S. Rana, R. Ahsan, and S. N. Ghani, "An optimized design of network arch bridge using global optimization algorithm," *Advances in Structural Engineering*, vol. 17, no. 2, pp. 197–210, 2014.

[17] A. Pipinato, "Structural optimization of network arch bridges with hollow tubular arches and chords," *Modern Applied Science*, vol. 12, no. 2, pp. 36–53, 2018.

[18] A. Pipinato, "Structural analysis and design of a multispan network arch bridge," *Proceedings of the Institution of Civil Engineers – Bridge Engineering*, vol. 169, no. 1, pp. 54–66, 2016.

[19] D. Ammendolea, D. Bruno, F. Greco, P. Lonetti, and A. Pascuzzo, "An investigation on the structural integrity of network arch bridges subjected to cable loss under the action of moving loads," *Procedia Structural Integrity*, vol. 25, pp. 305–315, 2020.

[20] C. D. Tetougueni, P. Zampieri, and C. Pellegrino, "Lateral Structural Behaviour of Steel Network Arch Bridges," in *Proceedings of the 7th ECCOMAS Thematic Conference On Computational Methods In Structural Dynamics And Earthquake Engineering*, M. Papadrakakis and M. Fragiadakis, Eds., pp. 5834–5841, Crete, Greece, June 2019.

[21] P. Zampieri, C. D. Tetougueni, E. Maiorana, and C. Pellegrino, "Post-buckling of network arch bridges subjected to vertical loads," *Structure and Infrastructure Engineering*, vol. 17, no. 7, pp. 941–959, 2020.

[22] F. Greco, P. Lonetti, and A. Pascuzzo, "Structural integrity of tied arch bridges affected by instability phenomena," *Procedia Structural Integrity*, vol. 18, pp. 891–902, 2019.

[23] P. Lonetti and A. Pascuzzo, "A practical method for the elastic buckling design of network arch bridges," *International Journal of Steel Structures*, vol. 20, no. 1, pp. 311–329, 2019.

[24] P. Lonetti, A. Pascuzzo, and S. Aiello, "Instability design analysis in tied-arch bridges," *Mechanics of Advanced Materials and Structures*, vol. 26, no. 8, pp. 716–726, 2019.

[25] F. M. Mato, M. O. Cornejo, and J. N. Sánchez, "Design and construction of composite tubular arches with network

suspension system: recent undertakings and trends," *Journal of Civil Engineering and Architecture*, vol. 5, no. 3, pp. 191–214, 2011.

[26] P. Tveit, "On Network Arches for Architects and Planners," 2012, http://home.uia.no/pert.

[27] P. Tveit, "Systematic Thesis on Network Arches," 2014, http://home.uia.no/pert.

[28] P. Tveit, "Information on the Network Arch by Per Tveit," 2016, http://home.uia.no/pert/index.php/Home.

[29] R. Belevičius, A. Juozapaitis, D. Rusakevičius, and D. Šešok, "Topology, shape and sizing optimization of under-deck stayed bridges," in *Proceedings of the Fourth International Conference on Soft Computing Technology in Civil, Structural and Environmental Engineering*, Y. Tsompanakis, J. Kruis, and B. H. V. Topping, Eds., Civil-Comp Press, Stirlingshire, U K, 2015.

[30] R. Belevičius, A. Juozapaitis, and D. Rusakevičius, "Parameter study on weight minimization of network arch bridges," *Periodica Polytechnica: Civil Engineering*, Budapest University of Technology and Economics, vol. 62, no. 1, pp. 48–55, 2018.

[31] R. Belevičius, A. Juozapaitis, D. Rusakevičius, and S. Žilėnaitė, "Parametric study on mass minimization of radial network arch pedestrian bridges," *Engineering Structures*, vol. 237, pp. 112182–112189, 2021.

[32] R. Belevičius, A. Juozapaitis, D. Rusakevičius, and S. Žilėnaitė, "Optimal schemes of radial network arch pedestrian bridges: an extensive dataset of solutions under different conditions," *Data in Brief*, vol. 36, pp. 107149–107218, 2021.

[33] C. Menn, *Prestressed Concrete Bridges*, Birkhauser Verlag, Vienna, Austria, 1989.

[34] MathWorks, "MathWorks," 2022, https://uk.mathworks.com/help/gads/genetic-algorithm.html.